Pure Appl. Geophys. 168 (2011), 521–541

DOI 10.1007/s00024-010-0127-8

Pure and Applied Geophysics

Some Contributions of the Neo-Deterministic Seismic Hazard Assessment Approach to Earthquake Risk Assessment for the City of Sofia

Ivanka Paskaleva,[1] Mihaela Kouteva-Guentcheva,[1] Franco Vaccari,[2,3] and Giuliano F. Panza[2,3]

Abstract—This paper describes the outcome of the advanced seismic hazard and seismic risk estimates recently performed for the city of Sofia, based on the state-of-the-art of knowledge for this site. Some major results of the neo-deterministic, scenario-based, seismic hazard assessment approach (NDSHA) to the earthquake hazard assessment for the city of Sofia are considered. Further validations of the recently constructed synthetic strong motion database, containing site and seismic source-specific ground motion time histories are performed and discussed. Displacement and acceleration response spectra are considered. The elastic displacement response spectra and displacement demand are discussed with regard to earthquake magnitude, seismic source-to-site distance, seismic source mechanism, and local geological site conditions. The elastic response design spectrum from the standard pseudo-acceleration, versus natural period, T_n, format, converted to a capacity diagram in $S_a - S_d$ format is discussed in the perspective of the Eurocode 8 provisions. A brief overview of the engineering applications of the seismic demand obtained making use of the NDSHA is supplied. Some applications of the outcome of NDSHA procedure for engineering purposes are shown. The obtained database of ground shaking waveforms and time-histories, computed for city of Sofia is used to: (1) extract maximum particle velocities; (2) calculate the space distribution of the horizontal strain factor $\text{Log}_{10}\,\varepsilon$; (3) estimate liquefaction susceptibility in terms of standard penetration test, *N* values, and initial over burden stress; (4) estimate damage index distribution; and (5) map the distribution of the expected pipe breaks and red-tagged buildings for given scenario earthquakes, etc. The theoretically obtained database, based on the simultaneous treatment of the data from many disciplines, contains data fully suitable for practical use. The proper use of this database can lead to a significant seismic vulnerability reduction and thus contributes to earthquake preparedness.

Key words: Seismic hazard, earthquake scenario, ground motion modelling, neo-deterministic hybrid approach, seismic demand, damage index and vulnerability.

1. Introduction

The region of Sofia, the main Bulgarian city, is among the areas exposed to the highest earthquake danger in the country. Although the historical earthquake record reports data on several strong damaging earthquakes that have occurred in this region, there are no instrumental records of seismic strong ground motion available for this region.

The city of Sofia extends over 1,315 km^2 with an urbanized territory of 242 km^2 and a population of about 1,397,000 ($\sim$2 million during the day). It is the major political, economic, scientific, culture, and transport centre of the country. Sofia is an industrial centre (800 large enterprises) yielding 50% of overall national industrial production, and a great number of industrial facilities of national importance form the infrastructure of the city. The high concentration of population and various activities of national importance, the variety of elements exposed to risk, and the high seismicity of the region make the problems of earthquake risk evaluation and mitigation of great importance. It is obvious that a strong earthquake could strike the city, and that the damage caused and co-seismic effects could result in a national disaster.

In the context of the state of the art, the major objectives of this paper are to contribute to seismic hazard assessment for Sofia, provide further validation of the neo-deterministic seismic hazard assessment, NDSHA, for the city of Sofia, and to illustrate the direct

[1] CLSMEE-BAS, 3 Acad. G. Bonchev str., 1113 Sofia, Bulgaria. E-mail: mkouteva@geophys.bas.bg
[2] DST-UNITS, Via E. Weiss 4, 34127, Trieste, Italy.
[3] ICTP, Trieste, Italy.

application of the outcome of NDSHA procedure to earthquake engineering purposes.

2. The Earthquake Record

The available information about ancient events is incomplete and uncertain and only approximate estimation of their location is possible. Published historical documents prove the occurrence of destructive earthquakes during the fifteenth to eighteenth centuries in the Sofia region (Watzov, 1902) and the largest earthquakes are those which occurred in 1818 with epicentral intensity I_o = VIII–IX MSK-64, in 1858 with I_o = IX–X (near Sofia), and in 1905 with $M \sim 6.5$ (near the town of Trun in the western marginal part of the Sofia region). The epicentral macroseismic intensity, $I_o \sim X$, summarising the heavy destruction in the town of Sofia in 1858, was first evaluated on the MSK64 scale (Petkov and Christoskov, 1965a, b) and updated later on the EMS98 scale (Paskaleva *et al.*, 2007). Here and in the following text, when non-integer values for the epicentral intensity are reported in the literature we use the symbol $\sim$ followed by an integer. In fact, any macroseismic intensity scale by its nature is a discrete scale of integer values. To be conservative, we round off by excess the non-integer values given in the literature. The scarcity of the data makes interpretation of that earthquake still disputable; moreover at that time (1858) Sofia was a small town with an urbanized area of ~ 2.8 km^2 and population less than 15,000 inhabitants. The strongest earthquake which has occurred in Sofia so far is the earthquake of October 18, 1917 with magnitude $M = 5.2$ (Kirov, 1952; Petkov and Christoskov 1965a, b) and reported epicentral intensity $I_o \sim$ VIII, MSK-64 (Petkov and Christoskov 1965a, b). Since 1917 strong earthquakes, magnitude $M > 5.0$, have not occurred in this region. Recently, in 15, November 2008, an earthquake of magnitude 4.0 hit Sofia without reported damage.

3. Seismic Hazard Assessment (SHA) and Seismic Microzonation Studies

In the last 15 years several studies on seismic hazard in Bulgaria (Bonchev *et al.*, 1982; Orozova-Stanishkova *et al.*, 1994, 1996; Simeonova *et al.*, 2006) have been published. These studies and particularly the investigation targeted on the Sofia region (Petkov and Christoskov 1965a, b; Christoskov *et al.*, 1989; Stanishkova and Slejko, 1991; Ranguelov, 1996; Ranguelov and Toteva, 1998; Solakov and Christoskov 2001), although based on different approaches, call the public's attention to the high earthquake danger within the Sofia region. Maximum macroseismic intensity at Sofia, I = IX (MSK), already observed in 1858 (Bonchev *et al.*, 1982) and, possibly, locally exceeded, can be expected to occur within a period of 150 years (Christoskov *et al.*, 1989). According to the seismic zoning map for 1,000-year return period, given in the Bulgarian Code for Design of Buildings and Structures in Seismic Regions (1987), Sofia belongs to a region of expected intensity IX on the MSK-64 scale.

Different seismic zones are considered to determine the earthquake hazard of Sofia and its vicinity. In general the seismogenic zones Kresna, Plovdiv, Negotinska Krayna, and Gorna Orjahovitza are considered to make the major contribution to the seismic hazard of Sofia. The city is also prone to the remote Vrancea seismic zone (Romania), the long-period elements of the built environment being particularly vulnerable to these events, for example the Vrancea quake of March 4, 1977 (VV AA, Brankov, 1983). The recent seismic hazard maps of the Circum–Panonian region (Panza and Vaccari, 2000) show that Sofia could suffer peak design acceleration DGA up to 0.6g, peak ground velocities (PGV) = 60–120 m/s, and peak ground displacements (PGD) = 15–30 cm, which correspond to macroseismic intensity from VIII to X (MSK-76) (Medvedev, 1977). In these maps, usually, shallow seismicity is considered (the hypocentral depth considered is 10 km for events with magnitude less than 7, and 15 km for larger events) and the computations are limited to epicentral distances shorter than 90 km. In the case of Vrancea events the computation has been performed over Romanian, Northeastern Croatian, and Hungarian territory and within a circle of 350 km radius centred on the Vrancea region. The hypocentral depth considered for Vrancea events is 90 km for magnitude less than 7.4, and 150 km for larger events.

The first attempt at seismic microzonation for Sofia is the map in terms of macroseismic intensity, MSK, published in 1965 by Petkov and Christoskov (1965a, b). This map was prepared by making use of the Medvedev's (1960) method and distinguishes the micro zones on the base of their rigidity coupled with the information available about the water table level. The Petkov and Christoskov (1965a, b) map is redrawn in Fig. 1a (B), where, within the territory of the city of Sofia, three zones with different macroseismic intensity, MSK, are distinguished. Some later studies (Paskaleva, 2002) show that, considering, in addition, the coseismic effects (e.g. land-sliding, liquefaction), the intensity still varies within the same interval $\Delta I = 2$, even if the intensity distribution within the investigated territory changes visibly, particularly in the south-western part of the region.

A further development in the SHA targeted at the city of Sofia seismic microzonation is the probabilistic SHA (PSHA), published by Solakov and Christoskov (2001). In this study the results, obtained from a sensitivity analysis of the PGA, keeping the same seismic source model and the same seismicity characteristics, and varying the standard deviations in the PGA attenuation mode, are discussed. A difference of up to 200% in the PGA value for a 1,000-year period was obtained, and this result has been related to the fact that regional, but not local, attenuation functions were used. A doubt comes from the fact that, in general, the regional data sets are not statistically significant; they are, therefore, unsuitable for representing very different seismotectonic styles that are not mixable, and usually attenuation functions are derived with the assumption of the same propagation model for all the events considered (Decanini *et al.*, 2001). The preliminary computations of the *b* value for the seismic zones, which can potentially affect the seismic hazard at Sofia, carried out by applying a maximum likelihood procedure (Molchan *et al.*, 1997), supply an explanation for the failure of PSHA application to Sofia region. To perform the computations, the Earthquake Catalogue for East and South-east Europe (Shebalin *et al.*, 1999) for the Bulgarian territory, the Romanian earthquake catalogue for Vrancea zone in Romania, ROMPLUS (Oncescu *et al.*, 1999; http://www.infp.infp.ro), and two tectonic models (Todorovska *et al.*, 1995; Paskaleva *et al.*, 2001) were considered. The preliminary estimates of these coefficients listed in Table 1 (taken from Slavov *et al.*, 2004) show quite large confidence intervals for the *b* value. The available data are rather limited and the statistical determination of the coefficients of the frequency–magnitude relationships (FMR) for these zones is affected by large uncertainties (Molchan *et al.*, 1997). More detailed analysis of the pitfalls of PSHA have recently been discussed and published by Klügel (2005), Wang (2005), Klügel *et al.* (2006) and Klügel (2007a, b). A brief comparative analysis of the classical SHA procedure with the neo-deterministic SHA (NDSHA), scenario-based, procedure, summarising the NDSHA limits and possibilities compared with the other two approaches, was published by Panza et al. (2008).

A preliminary analysis of the site response in the Sofia region based on the definition of the elastic eigenfrequencies of the site, defined using the data

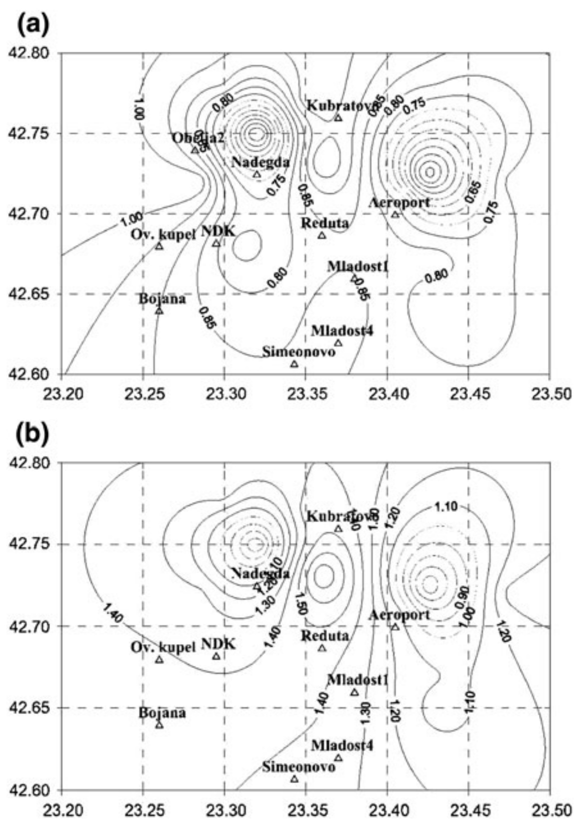

Figure 1

a Site response estimation at Sofia: distribution of the fundamental free period, Model_{30} (30 m depth). **b** Site response estimation at Sofia: distribution of the fundamental free period, Model_{50} (50 m depth)

Table 1

Estimates of the b coefficient of the FMR (taken from Slavov *et al.,* 2004*)*

Seismic zone	Tectonic model 1	Tectonic model 2
Sofia	0.50 ± 0.30	0.55 ± 0.33
Negotinska Krayna		1.01 ± 0.50
Kresna	0.69 ± 0.08	0.72 ± 0.08
Plovdiv	0.73 ± 0.08	0.76 ± 0.10
Gorna Orjahovitza	0.80 ± 0.20	0.76 ± 0.23
Vrancea	0.65 ± 0.15	0.70 ± 0.15

obtained from 14 boreholes, reaching depths up to 600 m, has been performed by Paskaleva (2002). Three models extending to different depths are used to perform these analyses: models M_{30} (30 m deep) and M_{50} (50 m deep) are based on the Eurocode 8 ground type classification and model $M_{\&}$ (reaching the depth of the bedrock identified with a shear velocity $V_s > 750$ m/s) is built by following the soil classification provided in the Bulgarian Code'87. The computations are performed applying the finite-element approach and the soil is discretised into one-dimensional finite shear elements, with viscous damping and lumped mass system. Maps of the first four free periods are obtained. The map of the fundamental free period for models M_{30} and M_{50} over the territory of the city are shown in Figs. 1a and b, respectively. The values of the fundamental natural period for the M_{30} model, shown in Fig. 1a are in the range 0.30–1.04 s, and for the M_{50} these values are in the range 0.90–1.40 s (Fig. 1b). The free periods obtained for the M_{50} model are 1.4–2 times larger than the corresponding M_{30} periods. These maps can be used only for preliminary practical preventive purposes, e.g. to keep the designers aware of the types of structural systems that should be avoided for a given location (Paskaleva *et al.*, 2004a).

The last attempts at a SHA via seismic wave propagation modelling for the purpose of seismic microzonation of Sofia and vulnerability estimation of the built stock (Paskaleva, 2002; Slavov *et al.*, 2004; Paskaleva, 2003; Paskaleva *et al.*, 2007, 2008; Dineva *et al.*, 2008) made use of an advanced innovative, scenario based NDSHA procedure (Panza *et al.*, 2001). Dineva and Paskaleva (2008) present a hybrid method, combining modal summation and boundary integral equations (MS-BIEM) for site-response estimation, using idealized 2D symmetric models. The results' validation in this study relies mainly on the comparative analyses of test examples considering both, MS-BIEM and MS-FD hybrid approaches (Dineva *et al.*, 2003), but no further validation on the case study of Sofia has been supplied. The other quoted studies (Slavov *et al.*, 2004; Paskaleva 2002; Paskaleva et al., 2008) rely on a hybrid approach (Fäh *et al.*, 1993, 1994a, b) that combines MS, applied for the seismic wave propagation modelling through the anelastic bedrock, representative of the wave travelling path from the source to the target site (Panza, 1985; Panza and Suhadolc, 1987; Panza *et al.*, 2001), and finite differences (FD) techniques (Virieux, 1984, 1986; Levander, 1988), applied to the anelastic, laterally inhomogeneous local medium around the site of interest, composed of sediments. The NDSHA hybrid procedure used for ground-motion modelling is capable of synthesising seismic ground motion from basic understanding of fault mechanism and seismic wave propagation. The capability of the procedure has already been proved, in the framework of UNESCO-IUGS-IGCP project 414, in several major cities in different regions: Bucharest (Panza *et al.*, 2002; Cioflan *et al.*, 2004), Thessaloniki (Triantafyllidis *et al.*, 1998), Zagreb (Lokmer *et al.*, 2002), Rome and Naples, Italy (Fäh *et al.*, 1995a; Vaccari *et al.*, 1995), Mexico City (Fäh *et al.*, 1995b), Beijing (Sun *et al.*, 1998; Ding *et al.*, 2004a, b). Despite the difficult verification of the synthetic strong motion database obtained, because of the lack of strong motion records in Sofia, some encouraging validation regarding the macroseismic intensity variation (Slavov *et al.*, 2004) and the seismic regulation prescriptions (Paskaleva *et al.*, 2008) have been performed. The hybrid approach is being increasingly used to constrain those aspects of ground motion prediction that are not constrained by recorded strong motion data, as in the case of Sofia City (Nenov *et al.*, 1990).

4. The NDSHA Procedure: Construction of the Synthetic Strong-Motion Database for the City of Sofia

To compute the synthetic seismic input, applying the NDSHA procedure (NDSHAP), it is necessary to:

1. Choose the controlling scenario earthquakes that are consistent with the seismicity, seismic regime, and seismic source mechanisms relevant for the target sites;
2. Define geophysical and geological properties along the path between the seismic sources and the target sites; and
3. Define as much as possible in detail the local geology of the target sites.

Therefore, the first step in the NDSHA is the choice of earthquake scenarios and the second step is to systemize the available geotechnical and geological information in order to construct the velocity model(s) for the bedrock structure, representative for the seismic wave propagation path from the seismic source to the target site and the local model(s), representative of the investigated site(s).

The available information on the earthquakes record has shown that two-thirds of the earthquakes had hypocentres no deeper than 10 km (Glavcheva *et al.*, 1996; Solakov *et al.*, 2001). Within this depth the whole energetic variety of the seismic sources is present, including the strongest known earthquake of 1858, $I_o \sim X$ and $M = 6.5$). One-sixth of the hypocentres occupy the depth range $10 < H < 25$ km, where it seems earthquakes with magnitude not larger than $M = 5$ occurred. The deepest seismic sources have been localized at depths of 30 km, where, again, mainly earthquakes with magnitude less than $M = 5$ occur. Following the empirical relationship available for the epicentral intensity versus magnitude (Lee *et al.*, 1990; Glavcheva, 1990) $I_o =$ IX and $M = 6.5$ correspond to an earthquake with focal depth $h = 10$ km while $I_o = X$ and $M = 6.5$ correspond to $h = 5$ m. Some other investigations estimate magnitude 7.0 for the 1858 earthquake (Christoskov and Sokerova 1987) and this value seems fully consistent with $I_o = X$, rather than IX. The earthquake scenarios considered to produce the database (Paskaleva et al. 2004a, b) correspond to a seismic source located 10 km west or southwards from the city centre (Christoskov *et al.*, 1987; Alexiev and Gerogiev 1997; Slavov, 2000, Matova, 2001; Solakov and Christoskov 2001). To construct the comprehensive earthquake scenarios, listed in Table 2, conservative combinations of information available in the literature (Alexiev 1997; Shanov *et al.*, 1998; Slavov, 2000) are considered. The computations for Sce1 ($M_w = 3.7$) and Sce2 ($M_w = 6.3$) consider the frequency-dependent response for point seismic source (Gusev, 1983). For the Sce3 and Sce3a ($M_w = 7.0$) the extended source with bilateral rupture propagation is considered, and the observation point is on a line at 90° from the rupture-propagation direction (Gusev and Pavlov, 2006).

The bedrock is represented by heterogeneous (in composition) and different (in age) rocks, which outcrop within the depression, because the city of Sofia is situated in the central southern part of the Sofia kettle, a continental basin in southern Bulgaria filled with Miocene–Pliocene sediments. The considered velocities of the longitudinal seismic waves in the Neogene sediments are of the order of 1,500–2,000 m/s, and for the basement are in the range 4,000–5,600 m/s. The documented significant lateral and vertical velocity heterogeneities are incorporated in the considered models. The Quaternary sediments,

Table 2

Scenario earthquakes used for the computations

Name of the scenario	Name of the geological profile	Magnitude M	Strike angle (°)	Dip angle (°)	Rake angle (°)	Focal depth (km)	Epicentral distance to the nearest profile (km)
Sce1	M1, M2, M3	3.7	340	77	285	2	8
Sce2	M1, M2, M3	6.3	340	77	285	10	10
Sce3	M1, M2, M3	7.0	340	77	285	10	10
Sce3A	M3	7.0	0	44	309	10	10

NB. The assumed source data, common to Sce 1, Sce2, and Sce3, correspond to the seismic event, which hit Sofia in 1858. Both focal mechanisms Sce3 and Sce3A are consistent with the available geological studies performed within the epicentral area (Christoskov and Sokerova 1987; Solakov and Christoskov 2001; Slavov *et al.*, 2004) representing the uppermost part of the geological sequence in the Sofia kettle region, are thick, from 3 to 100 m and more (Frangov and Ivanov, 1999). The three velocity layers that are distinguished in the sedimentary complex (Neogene and Quaternary sediments) on the territory of the town of Sofia (Ivanov, 1997), a top one with depth of 3–4 m (depending on the ground water level) with velocity of the longitudinal waves of 300–400 m/s; an intermediate one at a depth of 15–90 m and a velocity of 1,300–1,800 m/s, and a lower one with a velocity of 1,850–2,100 m/s were used to construct the local models. These models also take into account the fact that the velocity of the longitudinal seismic wave distribution sharply increases from 1,850–2,100 to 4,800–5,200 m/s at the boundary between the Neogene sediments and the basement. The man-made fill deposit layer is composed of old structures, technogenic soils, and industrial and household waste. This layer reaches its maximum thickness (up to 10 m) in the central parts of the town. The bulk density of the Quaternary sediments is about 1,840–2,070 kg/m^3. The unconsolidated Neogene sediments (sands, clays, clay sands, alevrolites, etc.) are characterized by a density not surpassing 2,000 kg/m^3. The density of the basement rocks (limestones, marls, sandstones, andesites, etc.) varies from 2,500 to 2,600 kg/m^3. Mean values of the geophysical properties of the geological strata representative for the Sofia kettle are given in Table 3. More details on the local site model used in computation of the seismic waveforms have recently been published by Paskaleva et al. (2004a, b, 2007).

A generalised scheme of the model adopted for the numerical experiments is drawn in Fig. 2a. Synthetic ground motions along three geological cross sections, M1, M2, and M3, described by different geometry of the representative geological strata were computed by Paskaleva *et al.* (2004b). These models correspond to the profiles 1A–1B, 2C–2D, and 3E–3F, respectively, and are shown schematically in Fig. 2b (C).

Several sets of synthetic accelerograms, velocigrams, and seismograms corresponding to sites 100 m apart along the considered geological cross sections, have been computed. The synthetic ground motion database (Paskaleva *et al.*, 2007) contains more than 2,700 signals, which have been grouped in three ranges of epicentral distances: 10–12, 12–16, and 16–20 km. For each group, mean ground motion spectral quantities are computed. Some validation via comparisons of the spectral quantities of the computed signals and the prescribed corresponding values in the acting seismic regulations is supplied by Slavov *et al.*, (2004) and by Paskaleva et al. (2008). Some additional considerations on the validation of the seismic input are given hereinafter.

4.1. Validation of the Bedrock Signal

The "worst" peak ground acceleration (PGA) distribution, obtained for the $M_w = 7$ scenario (Scenario 3a, model M3, Table 2), is shown in Fig. 3. In the same figure, the horizontal and vertical acceleration limits, according to the present Bulgarian code for design of buildings and structures in seismic regions, are shown as straight lines. The PGA values prescribed in the Bulgarian Code'87 are regarded as normative values. According to this figure, for epicentral distances less than 15 km the PGA does not exceed the normative acceleration values

Table 3

Mean values of the geophysical properties of the geological strata representative for the Sofia Kettle

Layer	Density	Seismic wave propagation velocities		Attenuation factor, Q	
	ρ (kg/m^3)	V_p (m/s)	V_s (m/s)	Q_p	Q_s
Soil layer	1,800	310	180	40	15
Quaternary cover	1,970	950	550	50	20
Tertiary sediments	1,920	1,400	800	75	30
Senonian marls	2,000	1,900	1,100	100	40
Triassic limestones	2,020	2,100	1,200	120	50
Senonian andesites	2,540	3,600	2,100	200	80

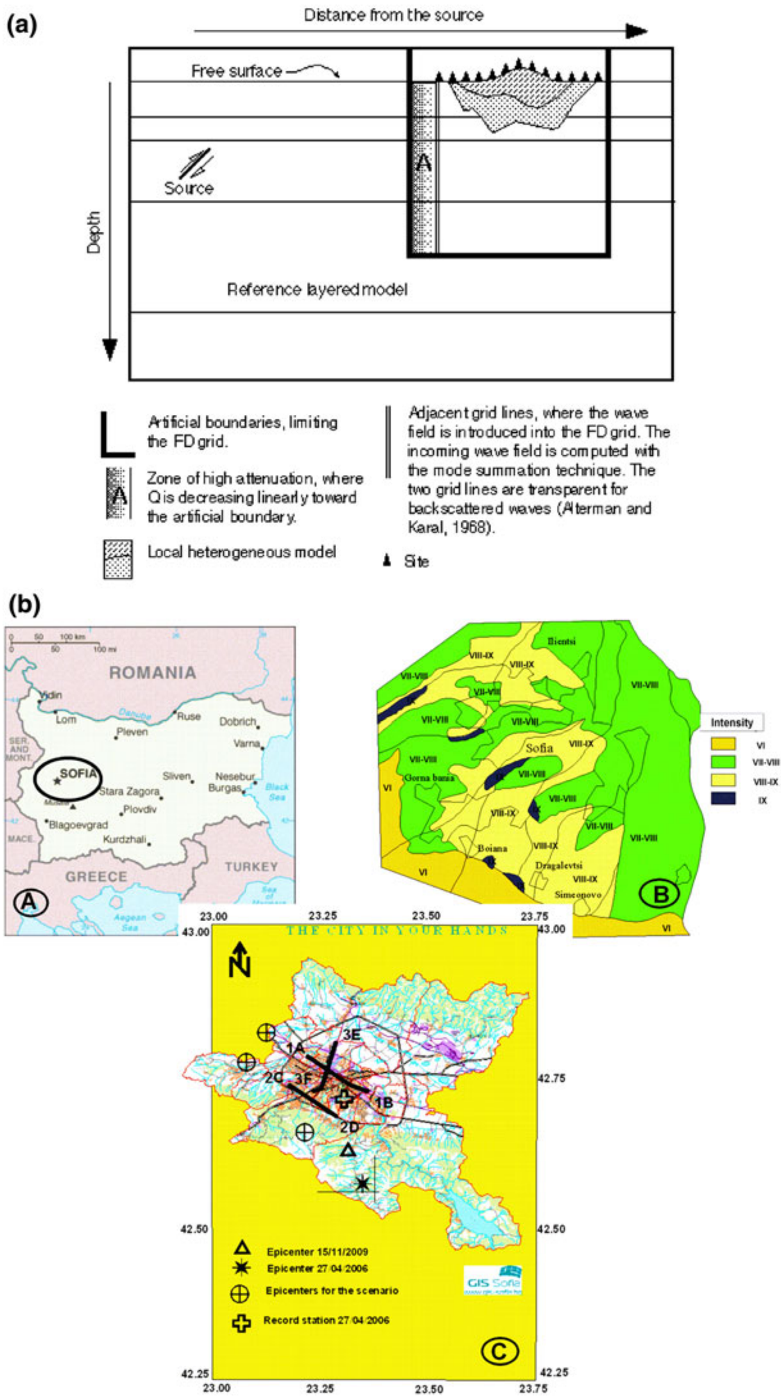

Figure 2

a A generalised scheme of the model adopted for the numerical experiments. **b** (*A*)*:* geographic location of the City of Sofia; (*B*): Redrawn Petkov and Christoskov (1965a, b) map; (*C*): city sketch with the location of the profiles used in the numerical simulations: 1A–1B and 2C–2D are parallel and are about 3.5 km apart. The ticks on the frame of the figure are: ⊕ locations of the epicentre for the scenario M = 7.0; ✷ - location of the epicentre for the scenario M = 3.7 (preliminary assessment) △ -location of the epicentre ML = 4.1 (preliminary assessment)

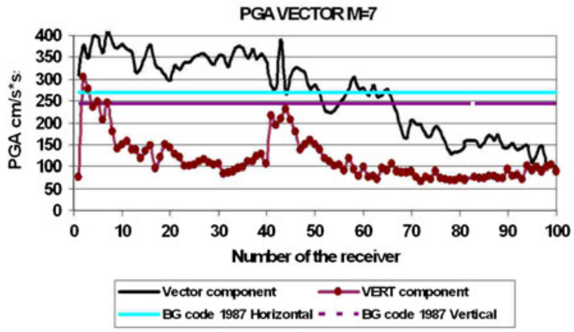

Figure 3
PGA resultant vector distribution along the profile, $M = 7$ scenario earthquake, $\mathrm{PGA}_{\mathrm{REZ}}=\sqrt{\mathrm{PGA}_{\mathrm{TRA}}^2 + \mathrm{PGA}_{\mathrm{RAD}}^2}$.

($K_c = 0.27g$ for horizontal components, $\mathrm{PGA}_{\mathrm{TRA}}$ and $\mathrm{PGA}_{\mathrm{RAD}}$, and $\mathrm{PGA}_{\mathrm{V}} = 0.9 \times 0.27g = 0.24g$, for the vertical). Some statistical estimates of the PGA distribution versus epicentral distance are given in Figs. 4a–c. For epicentral distances above 16 km, the PGA values, mean and mean +1 standard deviation, exceed the normative acceleration values. For the vertical component, the PGA values, mean and mean +1 standard deviation, become smaller than the normative ones for epicentral distances larger than 12 km.

The synthetic seismic signals are computed for the period range 0–10 s. The period interval 0–4 s has been chosen as the most interesting for engineering practice, and comparison of the computed displacements response spectra with the EC 8 ones has been performed over this period. The comparison of the computed displacement design spectra (SDD (T)) with the recommended EC8 design spectra (Fig. 5a, b) show that the synthetic spectral values for all models follow the EC8 amplitudes for the period range $T = 0.05$–1 s. The synthetic amplitudes are larger than the EC8 ones for periods $T = 1$–2 s.

Going further with the processing of the computed synthetic data, elastic displacement and acceleration response spectra for 5% damping have been determined from the synthetic accelerograms. Generalized resultant horizontal response spectra have been computed as the square root of the sum of the squares of the two horizontal components, $\mathrm{SA}_{\mathrm{REZ}}(T) = \sqrt{\mathrm{SA}_{\mathrm{TRA}}(T)^2 + \mathrm{SA}_{\mathrm{rad}}(T)^2}$. The important effect of the source-to-site distance, d_s, the

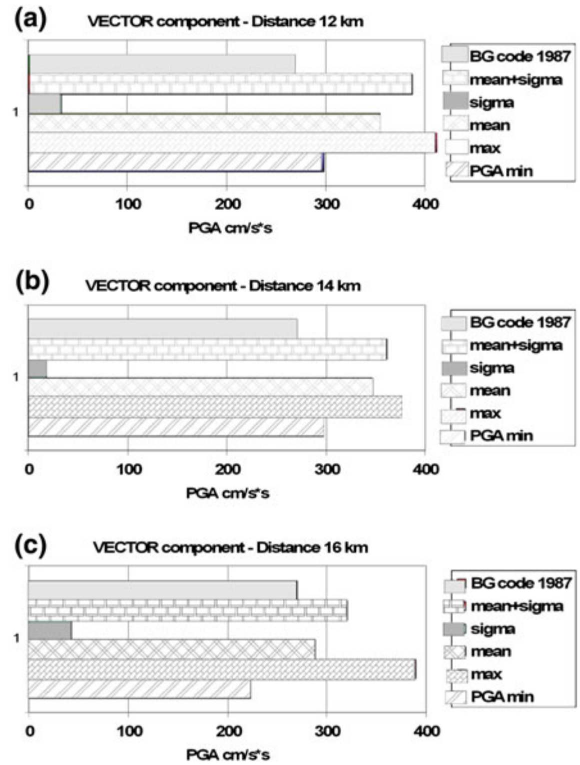

Figure 4
a PGA statistics versus epicentral distance, $M = 7$ scenario earthquake, $\mathrm{PGA}_{\mathrm{REZ}}=\sqrt{\mathrm{PGA}_{\mathrm{TRA}}^2 + \mathrm{PGA}_{\mathrm{RAD}}^2}$, epicentral distances 0–12 km. **b** PGA statistics versus epicentral distance, $M = 7$ scenario earthquake, $\mathrm{PGA}_{\mathrm{REZ}}=\sqrt{\mathrm{PGA}_{\mathrm{TRA}}^2 + \mathrm{PGA}_{\mathrm{RAD}}^2}$, epicentral distances 12–14 km. **c** PGA statistics versus epicentral distance, $M = 7$ scenario earthquake, $\mathrm{PGA}_{\mathrm{REZ}}=\sqrt{\mathrm{PGA}_{\mathrm{TRA}}^2 + \mathrm{PGA}_{\mathrm{RAD}}^2}$, epicentral distances 14–16 km

magnitude, and the local geological conditions on the spectral displacements is shown in Fig. 6, where the mean elastic displacement spectra along the three investigated models M1, M2, and M3, considering the scenario earthquakes given in Table 2, are plotted for the period range 0–2.5 s.

The elastic displacement spectral amplitudes in the near field ($d_s = 10$–12 km) are larger than those obtained for the far field for the three models, when considering earthquake scenarios Sce 1 ($M_w = 3.7$) and Sce 2 ($M_w = 6.3$). A similar trend is observed for model M1, Sce 3 ($M_w = 7.0$). The results obtained for model M2, Sce 3 ($M_w = 7.0$) and model M3, Sce 3 and Sce 3a ($M_w = 7.0$) show that the local geological conditions determine the seismic input

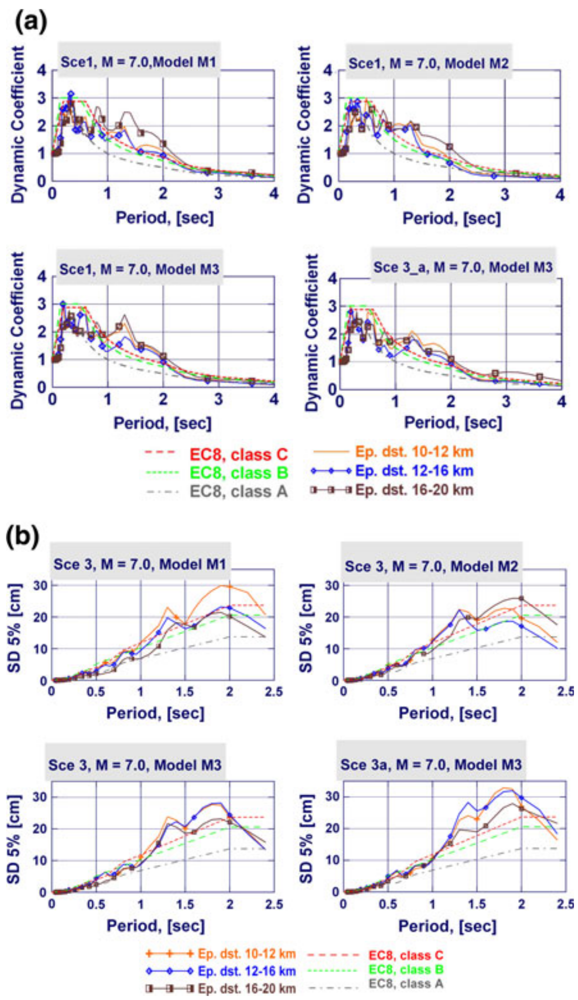

Figure 5

a Comparison of the computed dynamic coefficients (SA(T)/PGA mean values) for magnitude $M_w = 7.0$ for all considered models M1, M2, and M3 and the design values recommended by the EC8. The *dashed line* graphs correspond to soil conditions class A (rock), class B (stiff soil), and class C (soft soil), respectively. **b** Comparison between the computed elastic displacement spectra (mean values of the elastic displacement response spectrum, 5% damping) for magnitude $M_w = 7.0$ for all considered models M1, M2, M3 and the design displacement spectra, recommended by the EC8. The *dashed line* graphs correspond to peak ground acceleration 270 cm/s^2 (BG code 1987) and soil conditions class A (rock), class B (stiff soil) and class C (soft soil)

(Fig. 6a). The graph in Fig. 6b shows the relevant effect of the seismic source mechanism on the spectral amplitudes, particularly at periods $T > 1.25$ s.

Comparison of the maximum displacement d_s and the corresponding corner period T_c, obtained in this study and the results of Decanini *et al*. (2003) for stiff soil (S1), at distances from the source less than 5 km and larger than 30 km, magnitude $6.5 < M < 7.1$, is shown in Fig. 7a, b. The agreement between the results derived from the data bank of recorded signals (Decanini *et al*., 2003) and the results obtained from the synthetic database compiled using the neo-deterministic approach is fully satisfactory for displacements and corner periods also.

4.1.1 *Relative Displacement Spectra Attenuation*

The concept of the displacement relative attenuation, expressed by Att, was introduced by Decanini *et al*. (2003) to evaluate the effect of the distance from the source to the particular site. For the spectral displacement SD, Att (relative attenuation) is given by the ratio: Att = $\{Sd_{si}(T)\}/\{Sd_{s0}(T)\}$, where $Sd_{si}(T)$ represents the spectral displacement value d_s considering intervals of distance ($10 < d_s < 12$ km, $12 < d_s < 16$ km, $16 < d_s < 20$ km) to the source; $Sd_{s0}(T)$ is the spectral displacement for the shortest distance ($d_s = 10$ km). Obviously, low Att values indicate fast attenuation and high Att values denote slow attenuation with distance. The effect of the magnitude, geological conditions along the profiles, and the seismic source mechanism on the relative displacement attenuation is illustrated in Fig. 8.

Generally, the displacement relative attenuation in the far field along all investigated models, considering all scenarios, is visibly faster than the attenuation in the near field. The fastest displacement relative attenuation has been observed for model M3 and the slowest for model M2. Analysing the relative displacement spectra along Model M1 (the left column in Fig. 8a), values of Att increase with increasing magnitude, more visibly at periods $T > 1$ s. The far field attenuation, $d_s > 16$ km, is visibly faster than the near field one. The significant contribution of the geological conditions to the earthquake site response and to the relative displacement attenuation at the site is illustrated by the comparison between the plotted displacement relative attenuation for model M1 (left columns in Fig. 6a), model M2 (middle column) and model M3 (right column). The last graph in Fig. 8b (lower right corner) shows the effect of the seismic source

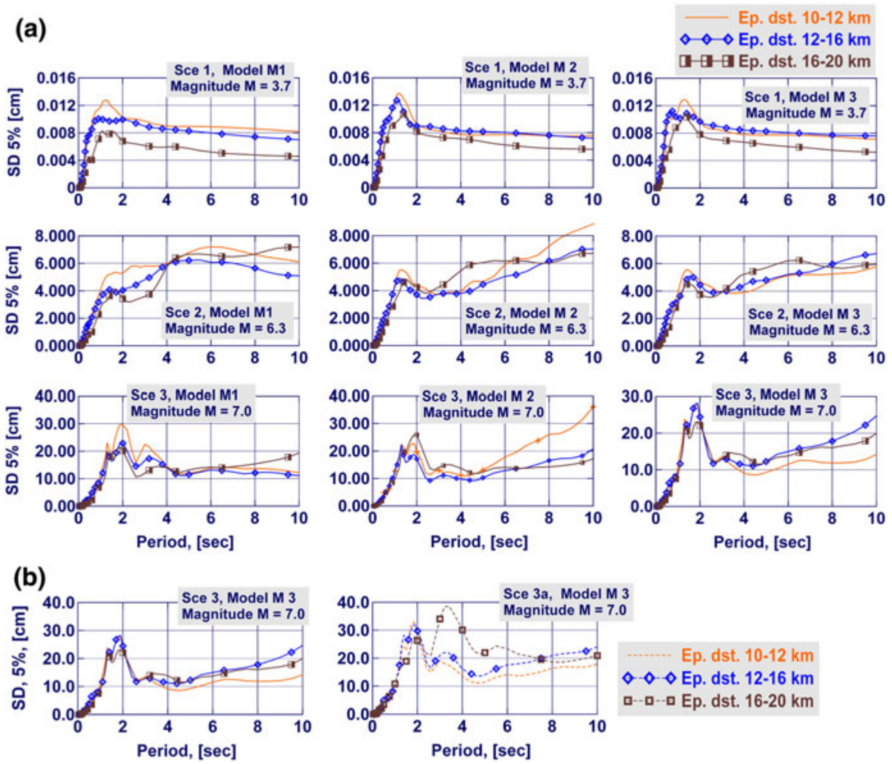

Figure 6

a Mean elastic displacement spectra computed for all considered models M1, M2, and M3 according to the scenario earthquakes listed in Table 2 (Sce 1, Sce 2, Sce 3). **b** Mean elastic displacement spectra computed for all considered model M3 according to the scenario earthquakes listed in Table 2. *Left* Sce 3 (*solid lines*), *right* Sce3a (*dashed lines*)

mechanism on the displacement relative attenuation for model M3—the displacement relative attenuation follows the same trend, but with larger amplitudes.

Figure 9 shows the comparison of the design displacements relative attenuation Att obtained from the synthetic database (computed for Sofia) with the Att values extracted from observations, e.g. as supplied by Decanini et al. (2003) and Bommer and Elnashai (1999). The attenuation coefficient obtained in this study, using the computed seismic input, shows visibly higher Att values, which indicate faster attenuation along the investigated site. This result calls our attention to the need to perform more parametric analyses in order to clarify the contribution of the different characteristics of the computation model and the input information to Att.

An extensive numerical analysis has been carried out on SDOF systems for natural periods T in the range 0–2 s. The elastic spectral displacement S_d and strength demand S_a, which represent the structural performance, have been extracted from all the computed accelerograms assuming a constant damping ratio of 5%. The results for earthquake scenarios $M = 7.0$ are plotted in $S_a - S_d$ format in Fig. 10. The same figure shows the comparison of the mean elastic acceleration–displacement diagram with the $S_a - S_d$ diagram, recommended in EC8, corresponding to the case-study of Sofia City—design acceleration $0.27g$ “B” soil conditions. The plot in Fig. 10 shows a good correlation between the compared data in the period range $0.4 < T < 0.8$ s, whereas for longer periods ($0.8 < T < 2.0$ s) the synthetic signals are dominant at all considered distances.

5. NDSHA: Engineering Applications

The NDSHA procedure supplies realistic waveforms of acceleration, velocities, and displacement of the free ground surface and thus it is possible to

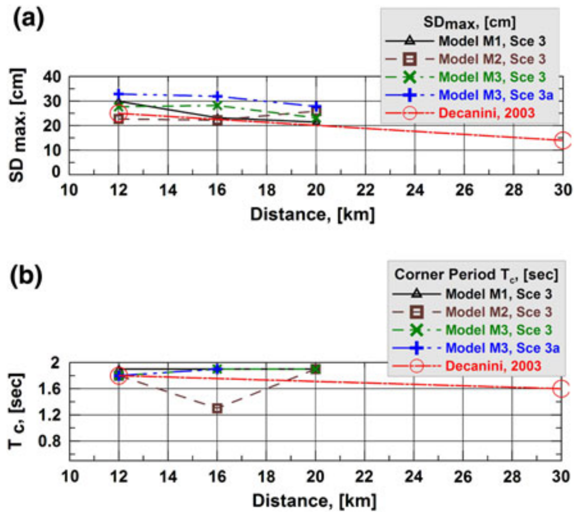

Figure 7

a Comparison of the maximum spectral displacement SD (models M1, M2, and M3) with the data of Decanini *et al*. (2003) for stiff soil (S1), magnitude range $6.5 < M < 7.1$. **b** Comparison of the corner period Tc corresponding to the maximum spectral displacement SD (models M1, M2, and M3) with the data of Decanini *et al*. (2003) for stiff soil (S1), magnitude range $6.5 < M < 7.1$

estimate from these signals, in a reliable way, any relevant variable used to characterize the ground motion for risk mitigation purposes. Obviously a similar wealth of information cannot supplied by PSHA. The synthetic data base, can be directly used for different engineering purposes, for example:

- provide seismic loading in terms of time series, consistent with both National Code and Eurocode 8 (2002) requirements;
- provide alternative definition of the seismic input, and particularly of the dynamic coefficient, for the National application of Eurocode 8;
- perform seismic microzonation and vulnerability estimates in terms of elastic and non-elastic quantities (only elastic quantities considered in this paper, non-elastic estimates will be the subject of another paper);
- perform surface strain and ground failure estimates, and preliminary liquefaction susceptibility estimates;
- proceed with capacitive and performance-based design;
- map space distribution of the damage index.

5.1. *Seismic Loading and Code Provisions*

The validation of the computed seismic demand against the seismic input, prescribed by the EC8, shown in Figs. 4, 5, 6, 7, 8 and 9 has shown the consistency of the computed seismic signals with the Code. Therefore this procedure is able to meet the requirements of the EC8 regarding the use of artificial accelerograms for description of the seismic motion and can be used as an optional independent generator of seismic input for earthquake engineering purposes. When strong motion instrumental records are lacking the NDSHA procedure can also be used as an optional independent procedure for definition of the seismic input in EC8 National Applications (e.g. considering an earthquake scenario with return period of 475 years).

The NDSHA procedure supplies site response estimates simultaneously in the frequency and space domains. The irregular pattern of the site amplification in the frequency–space domain, obtained even when considering rather simplified geological settings, as for the Russe case study, e.g. Kouteva et al. (2004), confirms the complicated properties of the so-called "site effect". The site response is because of the complex evolution of the seismic wave field (while it propagates through the laterally heterogeneous, geological media) that cannot be captured by standard convolutive methods as described for instance by Reiter (1990). In cases when the investor's technical specification requires, particularly, the use of software, based on the traditional PSHA or DSHA and the signal convolution, the NDSHA result pertinent to the bedrock should be used for "calibrating" or scaling the (bedrock) signal, that will have to be propagated through the model representing the local site conditions.

5.2. *Seismic Microzoning and Vulnerability*

The NDSHA can be used directly for seismic microzoning purposes. The seismic microzoning assigns the obtained seismic input, in terms of spectral acceleration (S_a), spectral displacement (S_d), or capacity diagram ($S_a - S_d$), to the area characterized by the corresponding local geological conditions (Paskaleva *et al.*, 2004b). For the

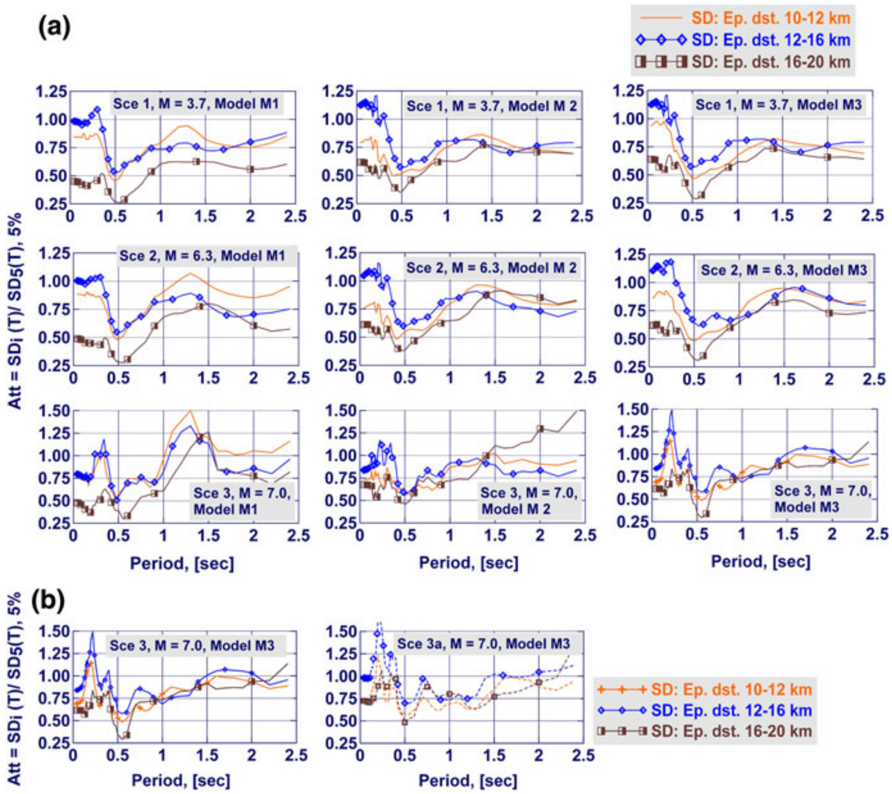

Figure 8

a Relative displacement spectra attenuation, computed along all investigated models M1, M2, and M3 considering scenarios Sce1, Sce2, and Sce3. **b** Relative displacement spectra attenuation, computed along investigated model M3 considering scenario Sce3a

discussed earthquake scenario Sce2, six homogeneous zones, shown in Fig. 10, can be identified. Average and maximum response spectra have been computed for each zone. The maximum response spectra, computed for 5% damping, for each of these zones are shown in Fig. 11 by solid lines whereas the thin line represents the BG code'87 design spectrum. For each spectrum the distance range *R* (km), measured from the beginning of the profile, where the spectrum is applicable, is specified. The maximum particle velocity for the zone is given as an indicator of the strain.

The available synthetic strong motion database can be readily applied to define site-specific design spectra based on average or maximum amplification. Such results have to be accounted for in site-specific design procedures, especially for underground lifeline systems, which are more sensitive to near surface strains than to maximum peak ground acceleration. This is a good starting point for the microzonation of Sofia. Many more cross-sections will be required to cover the whole city, for better understanding and estimation of the maximum expected risk (Paskaleva *et al.*, 2007). The NDSHA can be also used for estimation of the vulnerability of different elements of the built environment (Paskaleva *et al.*, 2007). The method can be used for the purpose of preliminary qualitative and detailed quantitative vulnerability assessments. In fact, all the performed validation of the theoretically obtained seismic input (S_a, S_d, $S_a - S_d$) has shown that the computed seismic demand is consistent with the Code prescriptions in the short period range, $0.05 > T > 1.0$ s, whereas it is characterized by visibly higher values of the variables considered for the longer periods $1 > T > 2.5$ s.

5.3. Surface Strain and Ground Failure Estimates

When records are scarce or non-existent as in the case of Sofia city, the synthetically generated

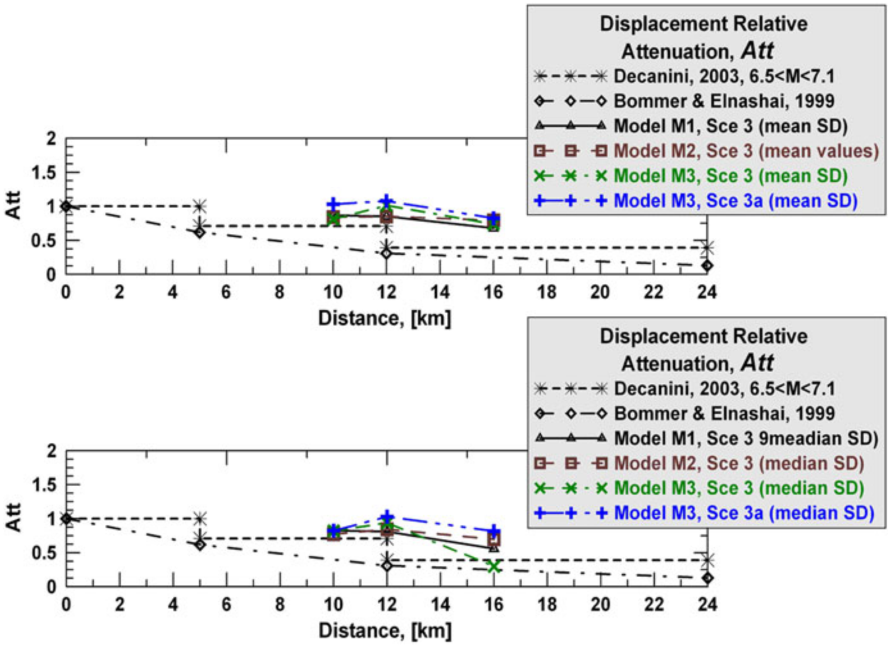

Figure 9
Relative attenuation coefficient Att. Comparison of the results obtained in this study for the generalized horizontal component (median values) with the data of DECANINI et al. (2003) ($6.5 < M < 7.1$) and BOMMER (1999) (magnitude-independent)

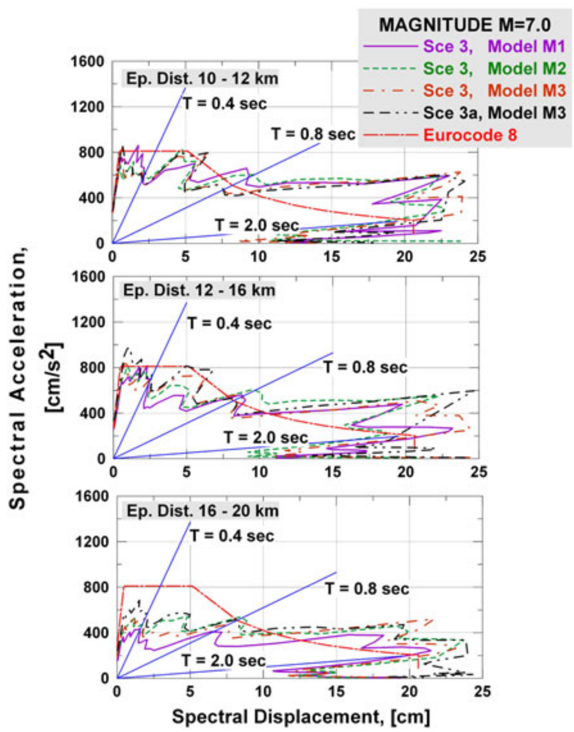

Figure 10
Elastic demand diagram. Comparison of the synthetics and the Eurocode 8 values

database, containing waveforms and time histories, can be directly used for prognostic estimates of the distribution of different data useful for design practice, urban planning, and earthquake preparedness. The computed velocities can be used to estimate the surface strain field and thus to make enable assessment of the expected number of red-tagged buildings and mean number of expected pipe breaks/km^2 as it has been done by PASKALEVA *et al*. (2004b). The map of the number of pipe breaks per km^2 for the city of Sofia, redrawn from PASKALEVA *et al*. (2004b), is shown in Fig. 12.

When considering long structures and their nonlinear response analysis, the designers have to pay particular attention to the representative surface strain and to the number of stress reversals that are related to the duration of the ground motion. The practice shows that for long in-plan structures (life-line systems, bridges, dams, etc.) the quasi-static deformation of the complete structure may contribute to the largest levels of the design loading. Therefore, every sound design approach has to consider all the relevant scaling data. The outcome of the NDSHA procedure in terms of ground surface velocities

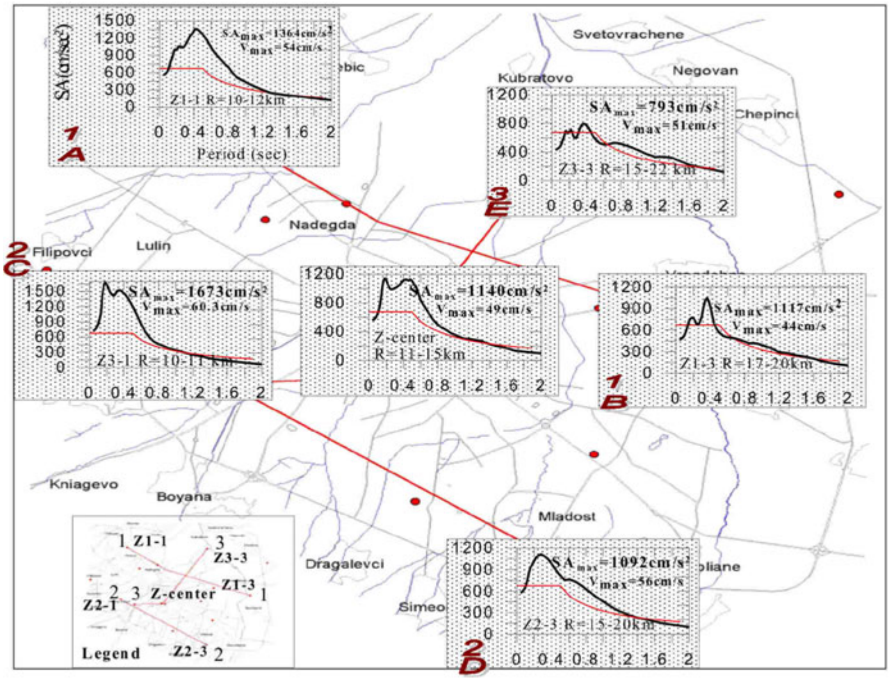

Figure 11

Maximum acceleration response spectra for the zones defined (*left corner* of the figure) for 5% damping. The *lines solid*, this study; *thin*, BG code'87 design spectrum; *R*, distance range, from the beginning of the profile, where spectrum is applicable

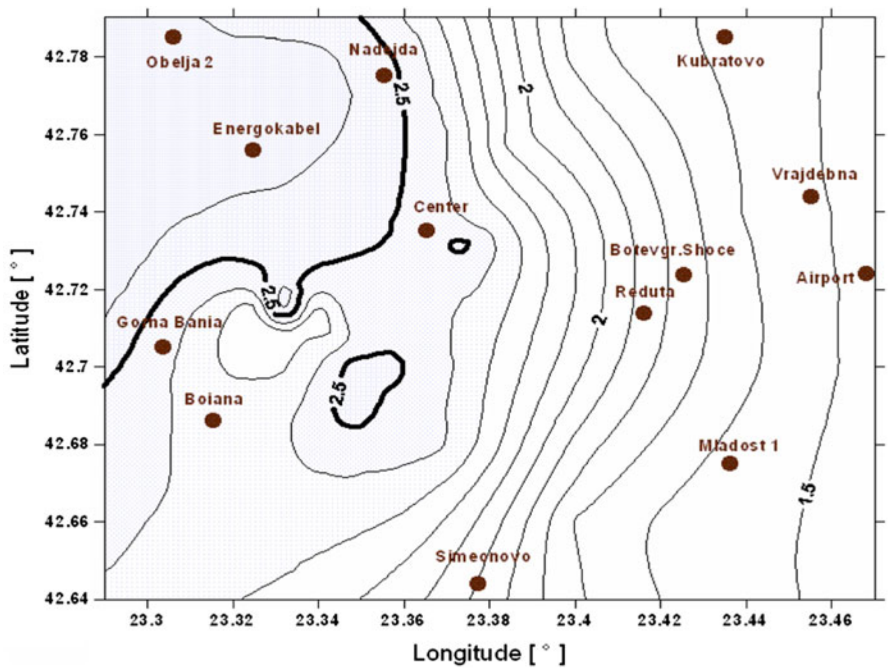

Figure 12

Sofia map of number of pipe breaks per km^2 compiled from synthetic velocigrams. The *solid line* indicates intensity higher than VIII (I_{MM}) (data from Trifunac and Todorovska, 1997) computed for the target sites allows us to estimate the peaks of the horizontal strain (ε) components, associated with the propagation of earthquake waves (PASKALEVA, 2002). The horizontal strain factor $\mathrm{Log}_{10}\,\varepsilon$ distribution, obtained as a result of the zonation of Sofia as computed by PASKALEVA (2002) is shown in Fig. 13, where the solid isoline −3.0 corresponds to the strain factor 10^{-3} beyond which a ground failure might be expected.

5.4. *Liquefaction Susceptibility*

The synthetic database based on the NDSHA procedure provides reliable values of all ground motion variables necessary for assessment of the liquefaction susceptibility, a very important aspect of the vulnerability (ROMANELLI *et al.*, 1998). An example dedicated to the city of Sofia, is given by Paskaleva (2002, 2008). The performed assessment, as shown in Fig. 14, should be treated as a general guide for the minimum level of liquefaction in Sofia city. Full liquefaction hazard assessment requires substantial engineering and professional judgment, looking site by site. The liquefaction analyses deal either with estimation of the shear stress expected during design earthquake motion or with assessment of the soil strength capacity in terms of the standard penetration tests, SPT, making use of different possible approaches (BERRILL and DAVIS, 1985; TRIFUNAC, 1995). PASKALEVA (2002) provides SPT estimates for the city of Sofia, shown in Fig. 14, that can be useful for various engineering and managing purposes concerning urban planning and earthquake preparedness.

5.5. *Seismic Demand and Capacitive Design Method*

Another aspect of the engineering application of the outcome of the NDSHA is related to its explicit representation of the seismic demand by an $S_\mathrm{a} - S_\mathrm{d}$ capacity diagram that can be the direct input for the capacitive design method. Dealing with the capacity design method, the representation of both the capacity (pushover) curve and the demand spectrum is made in the spectral acceleration (S_a, ordinate), spectral displacement (S_d, abscissa) coordinate

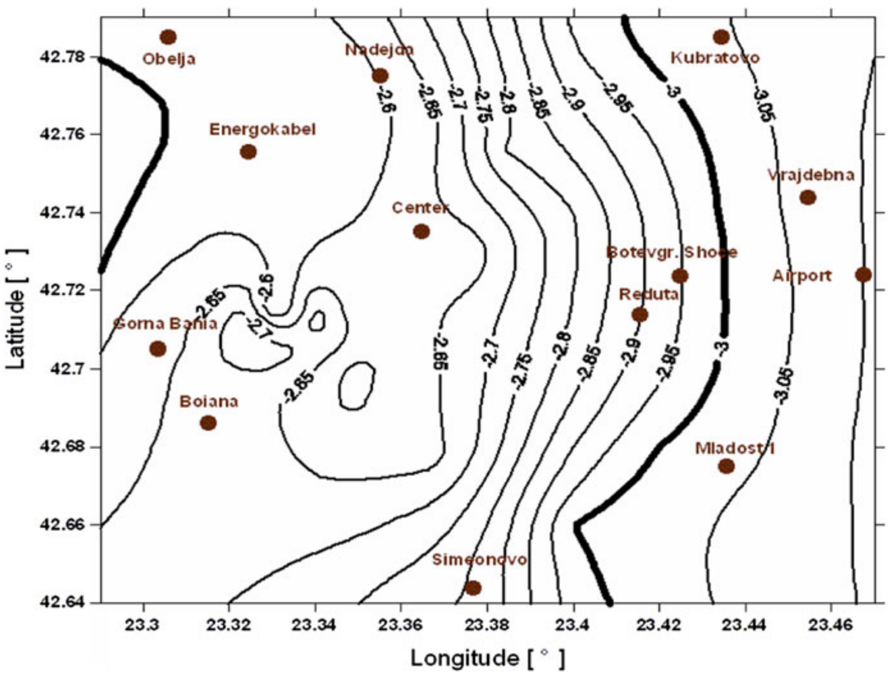

Figure 13
Horizontal strain factor $\mathrm{Log}_{10}\,\varepsilon$ distribution, obtained as a result of the zonation of the city of Sofia. The *solid* isoline −3.0 corresponds to the strain factor 10^{-3} beyond which a ground failure might be expected

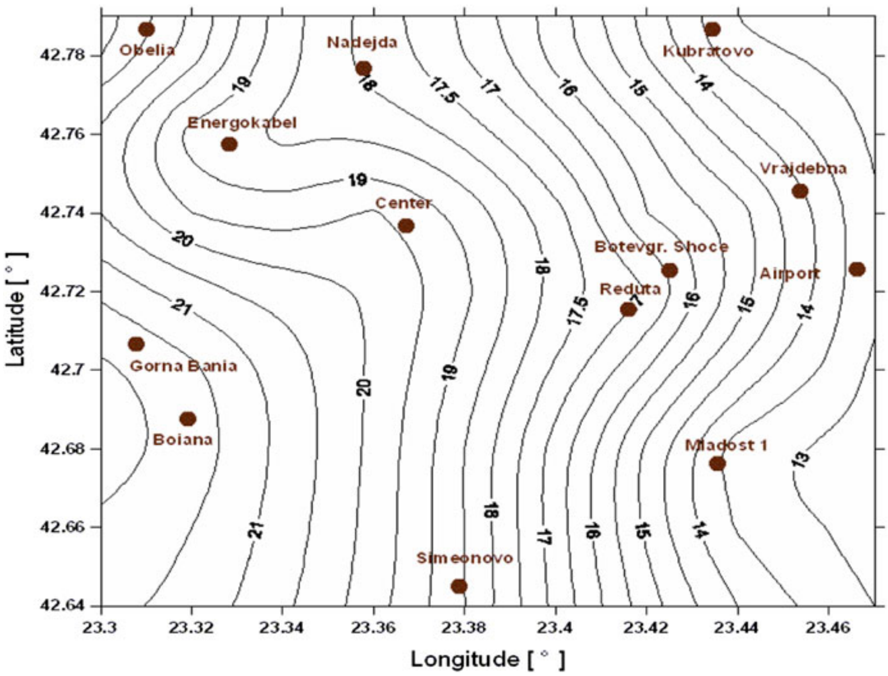

Figure 14
Maximum SPT, $\overline{N}$ values for Sofia supposing overburden pressure $\sigma_0 = 25$ kPa (Paskaleva 2002, 2008)

system. Capacity curves are based on engineering data (design, yield, and ultimate structural strength levels) characterizing the nonlinear behaviour of different classes of model building. They distinguish between construction materials, construction tradition, experience and technology used, and prescribed (by code) and achieved (in practice) levels of seismic protection. Further the capacity models are converted in capacity spectra and thus they can be overlapped with the seismic demand capacity diagram in order to define the performance point of the selected structure. Recently, in 2004, the conclusion of the RISK-EU Project (2004) made available for the public capacity models and capacity spectra for a large set of structures, representative of different typologies, time of design and construction, and number of storeys. Fragility curves are also supplied. Coupling the seismic demand capacity, computed for the city of Sofia with the information on the capacity spectra and the fragility curves for the set of structures considered by the RISK-EU Project enable estimation of the vulnerability of the existing built stock. Such analysis should be targeted by a separate study. It can provide very useful results that can be used for retrofit planning or insurance purposes and will be the subject of a separate study.

5.6. Space Distribution of the Damage Index

The synthetic seismic input, supplied by the NDSHA for the city of Sofia, is used for engineering purposes to assess the distribution of the damage index over the territory of the city, which is useful for urban planning, retrofitting of the built environment, the insurance industry, earthquake preparedness, earthquake risk reduction and earthquake risk management (Paskaleva *et al.*, 2007). These results are based on the seismic vulnerability analysis of a cast-in-situ single-storey industrial reinforced concrete (RC) frame that is designed and tested in the European Laboratory for Structural Assessment (ELSA) of the Joint Research Centre (JRC) of the European Commission at Ispra in the framework of the research project ''Seismic behaviour of reinforced concrete industrial buildings'' (Dimova and Negro, 2005a, b) The results, obtained in this study, have shown that even for relatively small changes in the source mechanism different values of the damage index (DI), are to be expected.

6. Conclusion

The city of Sofia is a typical example of a large city that is located in a seismic area and can suffer serious damage because of soil conditions, with deep soil deposits and severe local site amplification (Paskaleva *et al.*, 2007). Sofia is exposed to a high seismic risk, because macroseismic intensities up to X (MSK-76) can be expected in the city. For this reason prediction of ground motion from large future earthquakes is very important for hazard mitigation. Sofia is located on thick sedimentary basins, and taking site response into account is essential for realistic predictions of ground motion. The lack of instrumental strong motion records and the high earthquake risk, made evident by the available published reviews of the regional and local seismicity, requires the use of an appropriate scenario-based approach for seismic hazard assessment and advanced ground motion modelling procedures for definition of the seismic input for the city. Currently, uncertainties exist regarding the methodology employed and the level of sophistication required, which determines the number of input data, and the development of these data for implementation. The NDSHA is applied in the case study of Sofia City to cope with the scarcity of data, which will not be overcome in the near future, because of the absence of a relatively dense accelerographs array. The verification of the results obtained and the validation (some with real strong ground records) that has been done for several major cities in different regions (Mexico City, Rome and Naples, Italy, Bucharest, Thessaloniki, Beijing, Zagreb, Russe and Sofia; references have already been given in this paper) allow us to recognize that ground motion prediction using the described NDSHA approach is particularly suitable for all the cases poorly constrained by recorded strong motion data and can be used to make denser (interpolate) the local ground motion information supplied by the instrument.

The capability of demand estimations for buildings exposed to seismic loading is a major challenge for the prognostic estimates of seismic building behaviour. The elastic demand information is very useful for the further development of the design procedures, incorporating different advanced sub-procedures, for example

1. specific serviceability level performance evaluation procedure; and
2. verification of the reliability of the buildings

representative of different structural systems, the reliability of which must be consistent with both the code provisions and developing analytical evaluation procedures capable of predicting building performance with reduced uncertainty. The challenge of urban hazard mapping is to predict the ground motion effects related to various sources, path, and site characteristics not just at a single site but also over an extended region, and to do so with an acceptable level of well placed confidence (reliability). Seismic zoning then consists of linking together site-by-site estimates of site response. SHA practice, either PSHA or DSHA, has shown that such an approach may significantly underestimate the amplitudes and durations of strong ground motion, with energy being trapped within sedimentary basins because of critical reflections and generation of surface waves at the edges of the basin. This shortcoming is not surprising if the poor physical foundations of both PSHA and DSHA are considered. The rapid increase in the development of efficient computational methods and procedures for modelling seismic wave propagation in laterally varying geological structures, combined with increased knowledge of earthquake sources, enables realistic modelling of local site (usually sedimentary basins) effects on the ground motion generated by scenario earthquakes. Analysis of well-recorded data from dense seismograph arrays, when available, can improve the quality of the results of NDSHA by reducing its uncertainties.

Site-specific ground response analyses of strong seismic motion, for example the computed ones making use of the NDSHA procedure, are currently required for the design of new components of civil infrastructure on deep and/or soft sedimentary deposits, and for the revision of seismic code provisions.

In this work it was shown that the NDSHA approach can be used for practical applications in the situation of extreme scarcity of strong motion seismic data, because it enables use of simulated ground motion time-histories, with solid physical roots, for generation of a statistically significant number of input data, adequate to define the validity of the uncertainty assessment analyses.

The analysed synthetic seismic signals are computed using available source and structural models; the provided site response estimates and seismic demand at Sofia because of the chosen earthquake scenarios can be directly applied to assessment of the vulnerability of structures. By means of parametric studies of the source focal mechanism and of the velocity model, it is shown that NDSHA is a powerful approach that may be regarded as fundamental when adding information to the multidisciplinary ''database'' that must be defined for microzonation purposes. Given a certain earthquake scenario, and an appropriate structural model based on detailed geological, geophysical and geotechnical data, it is possible to evaluate, reliably, the local amplification in the frequency range of interest for civil engineering, and to obtain valuable data for the seismic microzonation.

The seismic demand supplied by the NDSHA application to the city of Sofia, together with the discussed engineering application, show that broadband ground motion simulations for different earthquake scenarios strongly contributes to reliable assessment of the earthquake-induced hazard in the Sofia urban area.

It is obvious that earthquakes will continue to occur and, if we are not prepared, to cause disasters. Assessing earthquake risk and improving engineering strategies to mitigate damage are the only viable options. The future availability of records of even moderate earthquakes will enable immediate validation and, when necessary, second-order revision of the first-order results obtained so far and already applicable to practice. The existence of the first-order reliable estimate of hazard given here enables timely updating of the estimate as new data become available.

Acknowledgments

CEI Projects "Deterministic seismic hazard analysis and zoning of the territory of Romania, Bulgaria and Serbia" and "Geodynamical Model of Central Europe For Safe Development Of Ground Transportation Systems", the bilateral cooperation between DST–UNITS, Trieste, Italy and CLSMEE–BAS, Sofia, Bulgaria, the Comune di Trieste and the CEI University network are gratefully acknowledged.

References

Alexiev, G., Georgiev, Tz. (1997), *Morphotectonics and seismic activity of the Sofia depression. Bulgarian Academy of Sciences*, J. Prob. Geogr. *1–2*, 60–69.

Berrill, J., Davis, R. (1985), *Energy dissipation and seismic liquefaction of sands, revised model, soils and foundations*, Jpn. Soc. Soil Mech. Found. Eng. *25*(2), 106.

Bommer, J. J., Elnashai, A. S. (1999), *Displacement spectra for seismic design*. J. Earthq. Eng. *3*(1), 1–32.

Bonchev, E., Bune, V., Christoskov, L., Karagyuleva, J., Kostadinov, V., Reisner, G., Rizikova, S., Shebalin, N., Sholpo, V., Sokerova, D. (1982), *A method for compilation of seismic zoning prognostic maps for the territory of Bulgaria*, Geologica Balkanica *12*(2), 3–48.

Brankov, G. (ed.), Vrancea Earthquake in 1977. Its after-effects in the People's Republic of Bulgaria. Publ. House of the Bulg. Ac. of Sciences, 1983, p. 428; Sofia (in Bulgarian).

Christoskov, L., Sokerova, D., and Rizhikova, Sn. (1987), *Catalogue of Historical Earthquakes in the Territory of Bulgaria* (Geophysical Institute of Bulgarian Academy of Sciences, Sofia).

Christoskov, L., Georgiev, Tz., Dineva, D., and Babachkova, B. (1989), *On the seismicity and seismic hazard of Sofia Valley*. In *Proc. 4th Int. Symp. 4–9 Sept.*, Bechine, pp. 447–453.

Cioflan, C.O., Apostol, B.F., Moldoveanu, C.L., Panza, G.F., Marmureanu, Gh. (2004), Deterministic Approach for the Seismic Microzonation of Bucharest, PAGEOPH 161, pp.1149–1164.

Decanini, L., Mollaioli, F., Panza, G. F., Romanelli, F., Vaccari, F. (2001), Probabilistic vs deterministic evaluation of seismic hazard and damage earthquake scenarios: a general problem, particularly relevant for seismic isolation. In *Proc. 7th International Seminar on Seismic Isolation, Passive Energy Dissipation and Active Control of Vibrations of Structures*, Assisi, Italy, October 2–5, 2001.

Decanini, L., Liberatore, L., Mollaioli, F. (2003), *Characterization of displacement demand for elastic and inelastic SDOF systems*, Soil Dyn. Earthq. Eng. *23*, 455–471.

Dimova, S. L., Negro, P. (2005a), *Seismic assessment of an industrial frame structure designed according to Eurocode. Part 1: experimental tests and their numerical simulation*, Eng. Struct. *27*, 709–723.

Dimova, S. L., Negro, P. (2005b), *Seismic assessment of an industrial frame structure designed according to Eurocode. Part 2: capacity and vulnerability*, Eng. Struct. *27*, 724–735.

DINEVA, P., VACCARI, F., PANZA, G. F. (2003), *Hybrid modal summation—BIE method for site effect estimation of a seismic region in a laterally varying media*, J. Theor. Appl. Mech. Bulg. Acad. Sci. *33*(4), 55–88.

DINEVA, P., PASKALEVA, I., LA MURA, C., PANZA, G. F. (2008), Hybrid MS-BIEM for seismic site-response phenomena: a case study of Sofia. In *Harmonization of Seismic Hazard in Vrancea Zone, NATO Science Security series* (eds. Zaichenco, Craifaleanu, Paskaleva) (Springer, Heidelberg) pp. 163–182.

DING, Z., ROMANELLI, F., CHEN, Y. T. and PANZA, G. F., (2004a). *Realistic modeling of seismic wave ground motion in Beijing city*. PAGEOPH *161*, 1093–1106.

DING, Z., CHEN, Y. T. and PANZA, G. F., (2004b), *Estimation of site effects in Beijing city*. PAGEOPH *161*, 1107–1123.

FÄH, D., IODICE, C., SUHADOLC, P., PANZA, G. F. (1993), *A new method for the realistic estimation of seismic ground motion in megacities: The case of Rome*, Earthq. Spectra. *9*, 643–668.

FÄH, D., IODICE, C., SUHADOLC, P., PANZA, G. F. (1994a), *Application of numerical simulations for a tentative seismic microzonation of the city of Rome*, Annali di geofisica *XXXVIII*, *5–6*, 607–615.

FÄH, D., SUHADOLC, P., MUELLER, St., PANZA, G. F. (1994b), *A hybrid method for the estimation of ground motion in sedimentary basins; quantitative modelling for Mexico city*, BSSA *84*, 383–399.

FÄH, D., IODICE, C., SUHADOLC, P., PANZA, G. F. (1995a), *Application of numerical simulations for a tentative seismic microzonation of the city of Rome*, Annali di Geofisica, *XXXVIII*, *5–6*, 607–615.

FÄH, D., SUHADOLC, P., MUELLER, St., PANZA, G. F. (1995b) *A hybrid method for the estimation of ground motion in sedimentary basins; quantitative modelling for Mexico City*, BSSA *84*, 383–399.

FRANGOV, G., IVANOV, Pl. (1999), Engineering geological modeling of the conditions in the Sofia graben and land subsidence prognoses. In *Proc. 4rth WG Meeting*, Dec. 3–6, 1999, Sofia, pp.17–13.

GUSEV, A. A. (1983), *Descriptive statistical model of earthquake source radiation and its application to an estimation of short period strong motion*, Geophys. J. R. Astron. Soc. *74*, 787–800.

GUSEV, A. A., PAVLOV. V. (2006), Wideband simulation of earthquake ground motion by a spectrum-matching, multiple-pulse technique. In *First European Conference on Earthquake Engineering and Seismology* (*a joint event of the 13th ECEE & 30th General Assembly of the ESC*). Geneva, Switzerland, 3–8 September 2006. Paper Number 408.

GLAVCHEVA, R. (1990), *Parametrization of the isoseismal from Bulgarian earthquakes*, Bulg. Geoph. J. *XVI*, *4*, 38–44 (in Bulgarian).

GLAVCHEVA, R., GEORGIEV, Tz., BOTEV, E., BABACHKOVA, Bl., TOTEVA, T. (1996), *Sofia graben and the earthquake of December 14 1995*, Bulg. Geophys. J. *XXII*, *3*, 44–50.

IVANOV, P., (1997), Assessment of the geological Conditions in the Sofia Kettle under seismic impact. In *Proc. International IAEG Conference, Athens, 1997*, Balkema, Rotterdam, pp. 1265–1270.

KIROV, K. (1952), A contribution to studying of the earthquakes in Sofia valley, An. Of main direction for geological and mine researches 5, 407–417 (in Bulgarian).

KLÜGEL, J.-U. (2005), *Problems in the application of the SSHAC probability method for assessing earthquake hazards at Swiss nuclear power plants*, Eng. Geol. *78*, 285–307.

KLÜGEL, J.-U., MUALCHIN, L., PANZA, G. F. (2006), *A scenario-based procedure for seismic risk analysis*, Eng Geol *88* 1–22, http://www.sciencedirect.com

KLÜGEL, J.-U. (2007a) *Error inflation in probabilistic seismic hazard analysis*, Eng. Geol. *90*, 186–192, http://www.sciencedirect.com.

KLÜGEL, J.-U. (2007b) Comment on "Why Do Modern Probabilistic Seismic-Hazard Analyses Often Lead to Increased Hazard Estimates" by Julian J. Bommer and Norman A. Abrahamson, BSSA *97*, 6. doi:10.1785/0120070018.

KOUTEVA, M., PANZA, G.F., ROMANELLI, F., PASKALEVA, I. (2004), *Modelling of the ground motion at russe site* (*NE Bulgaria*) *due to the Vrancea earthquakes*. J. Earthq. Eng. *8*, 2, 209–229.

LEE, V., PASKALEVA, I., CAO, H. (1990), *A note on the attenuation of seismic intensity in Bulgaria and Romania*. Soil Dyn. Earthq. Eng. *9*, No3, 151–161.

LEVANDER, A. R. (1988), *Fourth-order finite-difference P-SV seismograms*, Geophysics *53*, 1425–1436.

LOKMER, I., HERAK, M., PANZA, G.F., VACCARI, F. (2002), *Amplification of strong-ground motion in the city of Zagreb, Croatia, estimated by computation of synthetic seismograms*, Soil Dyn. Earthq. Eng. *22*, 105–113.

MATOVA, M. (2001), Recent manifestations of seismotectonic activity in Sofia region and their land subsidence potential. In *Proc. Final Conf. of UNESCO—BAS Project on Land Subsidence*, June 27–30, Sofia, pp. 93–98.

MEDVEDEV, Sv. (1960), *Seismic Engineering*. Moscow (in Russian).

MEDVEDEV, S. V. (1977), *Seismic intensity scale MSK—76*, Publ Inst Geophys Pol Acad Sci *117*, 95–102.

MOLCHAN, G., KRONROD, T., PANZA, G. F. (1997), *Multi-scale seismicity model for seismic risk*, BSSA *87*, 5, 1220–1229.

NENOV, D., PASKALEVA, I., GEORGIEV, G., TRIFUNAC, M. (1990), CATALOG of strong earthquake ground motion data in EQINFOS: Accelerograms recorded in Bulgaria between 1981 and 1987. Report No CE 90-02 (Sofia and Los Angeles, 1990, published in Southern California University).

ONCESCU, M. C., MARZA, V. I., RIZESCU, M., POPA, M. (1999), *The Romanian Earthquake Catalogue between 984–1997, in "Vrancea Earthquakes: Tectonics, Hazard and Risk Mitigation* (eds. F. WENZEL, D. LUNGU and (co-ed) O. NOVAK) (Kluwer, Dordrecht, Netherlands). Catalog under continuous update, pp. 43–47.

OROZOVA-STANISHKOVA, I., SLEJKO, D. (1994), Seismic hazard of Bulgaria, Nat Hazards *9*, 247–271.

OROZOVA-STANISHKOVA, I., COSTA, G., VACCARI, F., SUHADOLC, P. (1996), Estimates of 1 Hz maximum accelerations in bulgaria for seismic risk reduction purposes, Tectonophysics *258*, 263–274.

PETKOV, I. and CHRISTOSKOV, L. (1965), *On Seismicity in the Region of the Town of Sofia Concerning the Macroseismic Zoning*, Ann Sofia Univ *58*, 163–179.

PANZA, G. F. (1985), *Synthetic seismograms: the Rayleigh waves modal summation*. J. Geophys. *58*, 125–45.

PANZA, G. F., SUHADOLC, P. (1987), Complete strong motion synthetics, in seismic strong motion synthetics. In *Computational Techniques* (ed. Bolt B. A.) (Academic Press, Orlando, Vol 4, 153–204.

PANZA, G. F., VACCARI, F. (2000), Introduction in seismic hazard of the Circum-pannonian region. In *Pageoph Topical Volumes* (eds. PANZA, G. F., RADULIAN, M., TRIFU. C.) (Birkhauser Verlag: pp. 5–10).

PANZA, G. F., ROMANELLI, F., VACCARI, F. (2001), *Seismic wave propagation in laterally heterogeneous anelastic media: theory* *and applications to the seismic zonation*, Adv. Geophys.*43*, 1–95.

Panza, G. F., Alvarez, L., Aoudia, A., Ayadi, A., Benhallou, H., Benouar, D., Bus, Z., Chen, Y., Cioflan, C., Ding, Z., El-Sayed, A., Garcia, J., Garofalo, B., Gorshkov, A., Gribovszki, K., Harbi, A., Hatzidimitriou, P., Herak, M., Kouteva, M., Kuznetzov, I., Lokmer, I., Maouche, S., Marmureanu, G., Matova, M., Natale, M., Nunziata, C., Parvez, I.A., Paskaleva, I., Pico, R., Radulian, M., Soloviev, A., Suhadolc, P., Szeidovitz, G., Triantafyllidis, P. and Vaccari. F., (2002), *Realistic modeling of seismic input for megacities and large urban areas* (*the UNESCO/IUGS/IGCP project 414*). Episodes *25–3*, 160–184.

Panza, G. F., Kouteva, M., Vaccari, F., Peresan A., Cioflan, C. O., Romanelli, F., Paskaleva, I., Radulian, M., Gribovszk, i K., Herak, M., Zaichenco, A., Marmureanu, G., Varga, P.' Zivcic, M. (2008), Recent achievements of the neo-deterministic seismic hazard assessment in the CEI region. In *Proc. of the 2008 seismic Engineering Conference, Reggio Calabria, Italy* 8–11.07.2008 (eds A. Santini and N. Moraci) (American Institute of Physics, Melville, New York, AIP Conf. Proc., Vol. 1020, pp. 402–413).

Paskaleva, I., Kouteva, M., Panza, G.F., Evlogiev, J., Koleva, N., Ranguelov, B. (2001). *Deterministic approach of seismic hazard assessment in Bulgaria; case study northeast Bulgaria—the town of Russe*, Albanian J. Nat. Tech. Sci.*10*, 51–71.

Paskaleva, I. (2002), A contribution to the seismic risk assessment of the Sofia City. Report on CNR-NATO program, 65, Announcement, 219.33, May–October 2002, p. 100.

Paskaleva, I. (2003), A note on peak velocities and surface strains associated with strong earthquakes on the territory of Bulgaria and case study for Sofia. *CD-ROM First international Conference Science and Technology for Safe Development of Life Line Systems, 4–5 Nov, 2003, Sofia.*

Paskaleva, I., Matova, M., Frangov, G. (2004a) Expert assessment of the displacements provoked by seismic events: Case study for the Sofia metropolitan area. PAGEOPH 2004, Topical Volume 161, N5/6, Birkhauser Verlag pp. 1265–1283 (19) Seismic Ground Motion in Large Urban Areas (eds Panza, G.F., Paskaleva I., Nunziata, C.).

Paskaleva, I., Panza, G. F., Vaccari, F., Ivanov, P. (2004b), *Deterministic modelling for microzonation of Sofia—an expected earthquake scenario*. Acta Geod. Geoph. Hung. *39* (2–3), 275–295.

Paskaleva, I., Dimova, S., Panza, G. F., Vaccari, F. (2007), *An earthquake scenario for the microzonation of Sofia and the vulnerability of structures designed by use of the Eurocodes*, J. Soil Dyn. Earthq. Eng. *27*,(11) 1028–1041.

Paskaleva, I., Kouteva, M., Vaccari, F., Panza, G. F. (2008), Application of the ne-deterministic seismic microzonation procedure in Bulgaria and validation of the seismic input against Eurocode 8. In Proc. of the 2008 Seismic Engineering Conference, Reggio Calabria, Italy 8–11.07.2008 (ed. A. Santini and N. Moraci) (American Institute of Physics, Melville, New York), AIP Conf. Proc., vol. 1020, pp. 394–402.

Petkov, I. and Christoskov, L. (1965), *On seismicity in the region of the town of Sofia concerning the macroseismic zoning*, Ann. Sofia Univ. *58*, 163–179.

Ranguelov, B. (1996), Seismicity and site effects on the Sofia valley district, In *Proc. 1st WG meeting, Oct. 31–Nov. 3, Sofia*, pp. 28–31.

Ranguelov, B. and Toteva, T. (1998), Recent seismicity observed around Sofia City, In *Proc. 3rd WG meeting, Dec. 2–5, Sofia*, pp. 7–9.

Reiter, L., *Earthquake Hazard Analysis* (Columbia University Press, New York, 1990, 254 pp.).

Romanelli, F., Nunziata, C., Natale, M. and Panza, G. F., (1998). Site response estimation in the Catania area. In *The Effects of Surface Geology on Seismic Motion* (eds Irikura. K., Kudo. K., Okada. H. and Sasatani. T.) (A. A. Balkema, Rotterdam) pp. 1093–1100.

Shanov, S., Tzankov, Tz., Nikolov, G., Bojkova, A., Kurtev, K. (1998), *Character of the recent geodynamics of Sofia complex Graben*. Rev. Bulg. Geol. Soc. *59*, part I, 3–12.

Shebalin, N., Leydecker, G., Mokrushina, N., Tatevossian, R., Erteleva, O., Vassiliev, V. (1999), Earthquake Catalogue for Central and Southeastern Europe 342 BC–1990 AD, (European Commission, Report No. ETNU CT 93-0087) (1999).

Simeonova, S. D., Solakov, D. E., Leydecker, G., Busche, H., Schmitt, T., Kaiser, D. (2006), *Probabilistic seismic hazard map for Bulgaria as a basis for a new building code*, Nat. Hazards Earth Syst. Sci. *6*, 881–887. http://www.nat-hazards-earth-syst-sci.net/6/881/2006/

Slavov, Sl. (2000), Ground Modelling in the City of Sofia (TRIL-ICTP), Visitor's report.

Slavov, Sl., Paskaleva, I., Vaccari, F., Kouteva, M., Panza, G. F. (2004), *Deterministic earthquake scenarios for the City of Sofia*, PAGEOPH *161*, N5/6, 1221–1237.

Solakov, D., Simeonova, St, Christoskov, L. (2001), *Seismic hazard assessment for the Sofia area*, Annali di Geofisica *44*, No3, 541–556.

Stanishkova, I. and Slejko, D. (1991), Seismic hazard of the main Bulgarian cities, In *Atti del 10o Convegno Annuale del Gruppo Nazionale di geologica della terra solida; Roma, 6–8 November*, pp. 123–134.

Sun, R., Vaccari, F., Marrara, F., Panza, G. F. (1998), *The main features of the local geological conditions can explain the macroseismic intensity caused in Xiji-langfu* (*Beijing*) *by the MS = 7.7 Tangshan 196 earthquake,* PAGEOPH *152*, 507–521.

Todorovska, M., Paskaleva, I., Glavcheva, R. (1995), Earthquake source parameters for seismic hazard assessment: examples of Bulgaria. In *Proc. 10th ECEE*, Vienna, Austria, pp. 2573–2578.

Triantafyllidis, P., Hatzidimitriou, P. M., Suhadolc, P., Theodulidis, N. and Pitilakis, K. (1998), Comparison between 1-D and 2-D site effects modelling. In *The Effects of the Surface Geology on Seismic Motion* (eds Irikura, K., Kudo, K., Okada H. and Sasatani, T.) (Balkema, Rotterdam, Vol. 2) pp. 981–986.

Trifunac, M. (1995), *Empirical criteria for liquefaction in sands via standard penetration tests and seismic wave energy*, Soil Dyn. Earthq. Eng. *14* (6) pp 419–426.

Trifunac, M. and Todorovska, M. (1997), *Northridge California, earthquake 1994: density of pipe breaks and surface strains,* Soil Dyn. Earthq. Eng. *16*, 193–207.

Vaccari, F., Nunziata, C., Fäh, D., Panza, G. F. (1995), Reduction of seismic vulnerability of megacities: the cases of Rome and Naples. In *Proc. 5th Int. Conf. on Seismic Zonation, EERI*, Oct., Nice, France, pp. 1392–1399.

Virieux, J. (1984), *SH–velocity–stress Finite-difference method: velocity-stress finite-difference method*, Geophysics, *49*, 1933–1957.

Virieux, J. (1986), *P–SV wave propagation in heterogeneous media: velocity-stress finite-difference method*, Geophysics *51*, 889–901.

Wang, Z. (2005), *Discussion on Klügel's J.-U. problems in the application of the SSHAC probability method for assessing earthquake hazards at Swiss nuclear power plants*, EngGeol, *78*, 285–307; Eng. Geol. *82*, 86–88.

Watzov, Sp (1902), Tremblements de terre en Bulgaria au XIX siecle, IMPR. DE L'ETAT, Sofia, Bulg., 95 (in Bulgarian).

International Projects:

RISK-UE-EVK4-CT-2000-00014 "An advanced approach to earthquake risk scenarios with applications to different European towns" Contract: EVK4-CT-2000-00014; WP4: Vulnerability of current buildings, WP13: Application to Sofia; http://www.risk-ue.net/

UNESCO-IUGS-IGCP Project 414 "Realistic Modelling of Seismic Input for Megacities and Large Urban Areas" (http://users.ictp.it/www_users/sand/unesco-414.html)

Seismic Codes and Regulations

Bulgarian Seismic Code for Design and Construction in Seismic Regions (1987), Sofia.

European Committee for Standardization (CEN). Eurocode 8—Design of Structures for Earthquake Resistance. Part 1: General Rules, Seismic Actions and Rules for Buildings. prEN 1998-1, Brussels, 2002.

(Received April 30, 2009, revised February 17, 2010, accepted February 21, 2010, Published online April 9, 2010)